nearest-neighbor central-force interactions in the high-temperature limit. The Ludwig approximation has offered a considerable simplification and we have been able to do the sums analytically. As we saw in Sec. IV, the Ludwig approximation gives exact values of some of the anharmonic sums and it underestimates the magnitudes of most of the other sums by about 18%. However, the magnitude of the second-order quartic anharmonic contribution is overestimated by about 20%. Though the Ludwig approximation gives a good estimate of the of the η^2 contribution, it overestimates the η^4 contribution by a factor of 1.9. The main advantage of this approximation lies in the fact that we can do the summations analytically. The Ludwig approximation, therefore, could serve as a check on the computed values of the anharmonic sums.

---

*Present address: Department of Physics, P.U. Regional Centre for Post-Graduate Studies, Rohtak, India.

[1] C. R. Brooks, J. Phys. Chem. Solids **29**, 1377 (1968); A. J. Leadbetter, D. M. T. Newsham, and G. R. Settatree, J. Phys. C **2**, 393 (1969).

[2] A. J. Leadbetter, J. Phys. C **1**, 1489 (1968).

[3] A. A. Maradudin, P. A. Flinn, and R. A. Coldwell-Horsfall, Ann. Phys. (N.Y.) **15**, 360 (1961).

[4] K. G. Aggarwal and K. N. Pathak, Phys. Lett. A **35**, 255 (1971).

[5] L. Van Hove, *Quantum Theory of Many-Particle System* (Benjamin, New York, 1961).

[6] R. C. Shukla and E. R. Cowley, Phys. Rev. B **3**, 4055 (1971).

[7] W. Ludwig, J. Phys. Chem. Solids **4**, 283 (1958).

[8] L. J. Sham, Phys. Rev. **139**, B1569 (1965).

[9] P. F. Choquard, *The Anharmonic Crystal* (Benjamin, New York, 1967).

[10] K. N. Pathak and Y. P. Varshni, Phys. Lett. A **28**, 539 (1969).

[11] J. W. Leech and J. A. Reissland, J. Phys. C **3**, 975 (1970); J. Phys. C **3**, 987 (1970).

[12] L. A. Girifalco and V. G. Weizer, Phys. Rev. **114**, 687 (1959).

PHYSICAL REVIEW B VOLUME 7, NUMBER 10 15 MAY 1973

Relativistic Energy Band Structure and Properties of γ-Uranium*

D. D. Koelling†
Magnetic Theory Group, Physics Department, Northwestern University, Evanston, Illinois 60201

A. J. Freeman
Physics Department, Northwestern University, Evanston, Illinois 60201
and Argonne National Laboratory, Argonne, Illinois 60439

(Received 7 November 1972)

The electronic band structure of the high-temperature phase of uranium has been determined by means of the symmetized relativistic augmented-plane-wave method. Six different crystal potentials (three atomic starting configurations, $5f^4 7s^2$, $5f^3 6d^1 7s^2$, and $5f^2 6d^2 7s^2$, each taken together with $\alpha = 2/3$ and $\alpha = 1$ approximations for exchange) were employed in the warped-muffin-tin approximation. The relativistic effects are found to be very important and result in $5f$ bands which overlap and hybridize strongly with the very broad "$7s$-p" and broad $6d$ bands (which in the absence of the $5f$ states are found to be those typical of a high-atomic-number transition metal). The nonrelativistic energy bands are found to be incorrect in many ways. A calculated density of states shows considerable structure reflecting the s-d-f hybridization and a relatively high density of states (1.45 states per atom eV) at the Fermi energy. The Fermi surface is found to be complicated and to consist of two hole and one electron surfaces.

I. INTRODUCTION

Of all the actinide metals, uranium is perhaps the most famous because of its early unique role in the field of atomic energy. As with the other actinides, its unusual electronic properties—ranging from magnetism (especially in the case of its dilute alloys and intermetallics) to superconductivity (when subjected to pressure at low temperature)—are not well known and even less well understood.[1,2] One major difficulty, both for the experimentalist and the theorist, is the large number of crystallographic transformations which the metal undergoes as a function of temperature and pressure; in addition to the three well-known phases—the orthorhombic phase, called α_0 ($T < 940$ K), the tetragonal β phase ($940 < T < 1048$ K), and the body-centered-cubic γ phase ($T > 1048$ K) which exists up to the melting point at 1405 K—there are several other transformations all in a small range of temperature around 43 K. The high-temperature γ phase, the simplest modification, may be studied at ordinary temperatures by the addition of molybdenum, which stabilizes the γ phase at room temperatures and below. Both of the high-temperature phases can be stabilized down to low temperatures and exhibit superconducting behavior at low temperatures.[3] For example, the critical temperature of γ-U stabilized with 2-at. % Pt (or Rh) is 0.8 K, while that of γ-U stabilized with 15-at. % Mo impurities is 2.1 K. From measurements of the isotope effect in γ-U, it was found that[4] $T_c \propto M^{\alpha}$ with $\alpha = -0.53 \pm 0.02$, which (unlike the case of α-U) is very close to the BCS value of -0.5. The observation of superconductivity in the stabilized γ phase (and its absence in α-uranium) has been attributed to the absence (or presence) of $5f$ electrons in the metal.[4] Thus the nature and role of $5f$ electrons in these metals is a subject of much interest. Finally, the lack of unusual magnetic properties in this metal has led to the view that U metal is quite different from the rare-earth metals and more like the transition metals.

The theoretical investigations of the electronic properties of uranium metal have been confusing, at best. The neutral-atom configuration [(radon core) $5f^3 6d 7s^2$] is expected to form conduction bands in the metal but, unlike the case of its rare-earth counterpart Nd (which has three $4f$ electrons in the metal), uranium exhibits no localized-moment behavior associated with the $5f$ electrons.[5,6] The pioneering qualitative theoretical studies of Friedel[7] used a model for U in its different phases which consisted of a narrow high-density band (considered as a $6d$-$5f$ hybrid) overlapping a broad ($7s$) conduction band. This proposed band structure was later criticized by Lehman[8] who pointed out that spin-orbit interactions cannot be neglected for narrow-band metals and questioned the lack of numerical calculations to bear out the appearance of the $7s$ band in Friedel's model. Calculations by Lehman[8,9] and also by Ridley[10] showed that the atomic $7s$ levels are pushed upward by several eV when the metallic state in U is formed from the atoms yielding an unoccupied $7s$ band which may be neglected from further consideration. In these estimates of the band structure, the $5f$, $6d$, and $7s$ atomic states do form bands: a narrow $5f$ band (with a width of the order of 1 eV), a broader $6d$ band (about 4–6 eV wide), and a much broader $7s$ band which, however, lies above the Fermi energy.

This paper reports on a detailed relativistic energy-band-structure study[11,12] of γ- (bcc) uranium metal using the symmetrized relativistic augmented-plane-wave (SRAPW) method.[13,14] (We have focused these first efforts on the high-temperature form of uranium metal because the higher symmetry permits us to perform the calculations with less effort and in order to be able to assess and evaluate results without the added complexities inherent in the low-temperature low-symmetry phases, i.e., convergence difficulties, large matrices, and resulting high computing times and costs, etc.) A number of detailed calculations have been performed using various choices of atomic configurations to make up the crystal potentials in the warped-muffin-tin (WMT) approximation[12] and several values of α, the exchange scale constant which enters as a coefficient of the free-electron, $\rho^{1/3}$, exchange approximation. Unlike the band structures cited above, we find that the $5f$ bands hybridize strongly with the very broad "$7s$-p" and broad $6d$ bands. In the absence of the $5f$ bands (removed in another calculation by artificial means), the remaining band structure resembles very closely that of a high-atomic-number bcc transition metal. The relativistic treatment is found to be essential for obtaining the correct band structure, as is seen by comparison with nonrelativistic results also given here and those obtained by Kmetko[15] and Hill.[16] The nonrelativistic calculations are shown to give only a crude representation of the actual band structure of the actinides: The ordering and separation of the bands is incorrect (the $7s$-like bands lie well above the $5f$ bands instead of below); the large spin-orbit splittings of the bands are missing and degeneracies have not been removed (allowing crossings instead of anticrossings); and the $5f$ bandwidth estimates are incorrect because the relativistic contraction of the core which causes $5f$ orbital expansion is absent.

Section II, which follows, discusses the question of proper atomic configuration, choice of exchange parameter α, and the warping of the muffin-tin potential. Section III presents results obtained with six different crystal WMT potentials (three atomic configurations—$5f^4 7s^2$, $5f^3 6d^1 7s^2$, and $5f^2 6d^2 7s^2$—each taken together with $\alpha = \frac{2}{3}$ and $\alpha = 1$ approximations for exchange), results when the $5f$ bands are artificially removed, results of a nonrelativistic band calculation, and various comparisons. A computed density of states $N(E)$ is given for the $5f^3 6d^1 7s^2$ ($\alpha = \frac{2}{3}$) calculation as is an estimated Fermi surface. The radial charge density of the $5f$ component at different energies is presented in Sec. IV and discussed in relation to the superconductivity of uranium.

II. CALCULATION PROCEDURE

The energy-band calculations were performed using the relativistic augmented-plane-wave (RAPW) method.[13] Wherever possible, the additional symmetry of the crystal was exploited by employing projection-operator techniques in a symmetrized RAPW code.[14] Not only did this reduce the cost of computation but automatically yielded the symmetry properties of the states (two of the major reasons for first studying the bcc phase).

A. Warped-Muffin-Tin Approximation

It is standard practice in an APW or Korringa–Kohn–Rostoker (KKR) calculation to approximate the model potential by one which has the form of a muffin tin,[17,18] i.e., one which is (i) spherically symmetric within nonoverlapping spheres about each lattice site and (ii) constant (flat) between the spheres. This approximation is a good one for an fcc or bcc lattice where very little electronic charge is found outside the muffin-tin spheres. However, as the atomic number increases, more and more charge is found in this "outside region." Further, since a study of the actinides involves other structures besides the fcc and bcc structures, we must consider using a less-stringent approximation. The calculations reported here have used a warped-muffin-tin approximation,[12,14,19–23] which removes the second requirement of the muffin-tin approximation: The potential between the spheres need not be constant. That is, the only approximation made to the model potential is to spherically average within nonoverlapping spheres. That is, if we write the potential with arbitrary shape as its muffin-tin approximation V_{MT} plus two corrections,[20] V_1 and V_2,

$$V(\vec{r}) \equiv V_{\mathrm{MT}}(\vec{r}) + V_1(\vec{r}) + V_2(\vec{r}), \tag{1}$$

where V_1 is defined to be zero inside the muffin-tin spheres and V_2 to be zero in the interstitial region, we will be neglecting only V_2. This breakup is a natural one as V_1 is most appropriately treated by a Fourier-series decomposition (warping) and V_2 by a spherical-harmonic decomposition (nonspherical terms). DeCicco and Slater[24] pointed out quite early that V_1 would have a much larger effect than V_2. Thus it is quite reasonable to consider the inclusion of V_1 without V_2—an intermediate approximation denoted as a "warped-muffin-tin" (WMT) approximation. It is worth noting that domination of the V_1 effects assumes a cubic symmetry. Thus one would have to reevaluate the approximation for a lower-symmetry crystal such as α-U.

This intermediate approximation is a convenient one for the APW method since V_1 is only nonzero where the basis functions are plane waves. Thus, one is merely augmenting the muffin-tin Hamiltonian with the Fourier coefficients of V_1:

$$\langle \vec{k}, s \mid H^{\mathrm{WMT}} \mid \vec{k}', s' \rangle = \langle \vec{k}, s \mid H^{\mathrm{MT}} \mid \vec{k}', s' \rangle + \delta_{ss'} V_1(\vec{k}' - \vec{k}). \tag{2}$$

(Note that this is not perturbation theory.) We do not discuss the inclusion of V_2 as it is a much smaller correction for the bcc form. While it has been included in a number of nonrelativistic calculations,[22,23] it would be more complicated to include in a relativistic calculation.

B. Dependence of Potential on Assumed Atomic Configuration

As in all *ab initio* calculations, the starting potential plays a decisive role unless the calculations are carried out to self-consistency. [For the actinides, the uncertainty as to the nature of the 5*f* electrons (localized vs itinerant) was thought to raise the question as to whether they should or should not be included in the band calculations and made questionable the meaning of self-consistency itself.] As is generally done, the crystal potential is constructed from a charge density which is a sum of free-atom charge densities centered about each lattice site. The Coulomb potential produced by such a charge distribution is easily obtained and the exchange interactions are approximated using the local statistical $\rho^{1/3}$ exchange approximations.[25–27] While it is amazing that this model potential should work so well (neglecting as it does all distortions caused by inserting the atoms into the crystal), this prescription has considerable respectability in light of its past successes, and so provides the natural starting point for a study of the actinides.

The actinide metals are expected to have a conduction band structure which is more complicated than that of either the transition metals or the rare-earth metals because of the unusual nature of their atomic structure. The electronic structure of atomic uranium consists of a radon core (with 86 electrons), a partially filled 5*f* shell (containing three electrons), and three valence electrons in the atomic 6*d* and 7*s* states (distributed as $6d^1 7s^2$). In the rare-earth metals an open 4*f* shell in the rare earth forms a narrow localized band located well below the *d* and *s* bands; these latter bands are exactly like those of transition metals. As we shall see, the 5*f* electrons in the uranium are not so well localized as the 4*f* orbitals in the rare earths, and so their itinerant nature makes them hybridize strongly with both the 6*d* and 7*s* bands.

Since there is some uncertainty as to the "correct configuration" in the metal (at least as regards the atomic charge densities to be used in making up the crystal potential), we compare the relative positions in the energy of the outer electrons of three configurations in Fig. 1. The striking features of this figure include the large separation in energy between the closed 6*s* and 6*p* shells, the large relativistic (spin-orbit) splitting of these states, and the close relative positioning of the three different valence shells. This behavior is in sharp contrast with the positioning of the valence electrons in the rare earths, where the atomic 5*d* and 6*s* states lie close to one another in

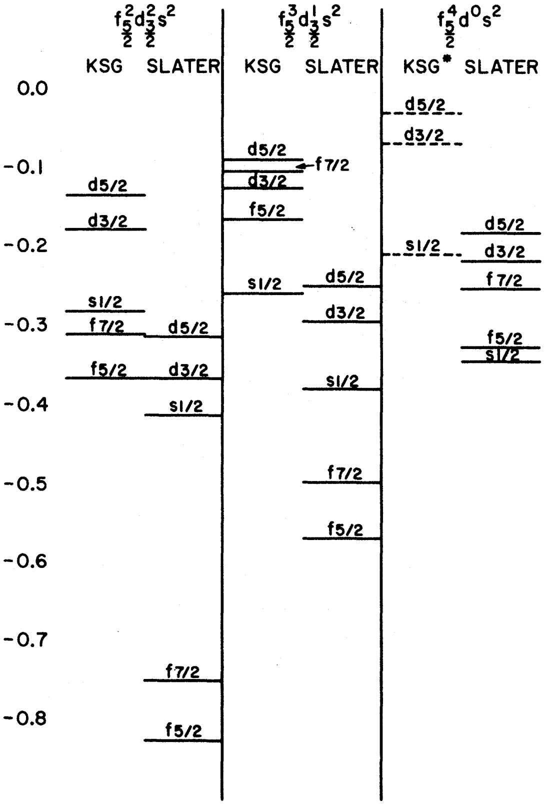

FIG. 1. Dirac-Slater atomic levels for uranium. Energy levels of the 5*f*, 6*d*, and 7*s* orbitals are given in rydbergs for three different assumed configurations, using both the Kohn–Sham–Gaspar (KSG) and Slater exchange approximations both with no Latter correction. The levels indicated for the f^4s^2 KSG calculation are the result of a linear extrapolation. Making this extrapolation, the 5*f* levels would not be bound by 0.05 Ry. Aside from an upward shift of 0.15 Ry, all the energy spacings resulting from the extrapolation agree well with the results of the calculation performed using a Latter correction.

energy and are widely separated from the 4*f* shell.[28] The crossing of the 6*d* and 7*s* levels by the 5*f*, as the number of such electrons is decreased, reflects the importance of Coulomb correlation effects (direct Coulomb and exchange) for these atomic electrons. From Fig. 1 one expects the 5*f* electrons to contribute to the conduction processes in the metal along with the 6*d* and 7*s* electrons. The large spin-orbit splittings demonstrate the importance of relativistic effects, which reflects the situation actually found for the metals. (The $6p_{3/2}$-$6p_{1/2}$ splitting is so large that in certain cases the $6p_{3/2}$ bands are found to overlap the bottom of the conduction bands.)

As a consequence of the uncertainty as to the appropriate atomic configuration (i.e., relative number of 5*f*, 6*d*, and 7*s* electrons), and in order to estimate the possible importance of self-consistency, we have done three band calculations in which the different atomic configurations (f^4s^2, $f^3d^1s^2$, and $f^2d^2s^2$) in U considered in Fig. 1 were used to generate starting crystal potentials. While there is a dependence of the computed band structure on the number of 5*f* electrons in the assumed potential, it is found to be somewhat smaller than the dependence of the bands on the exchange approximation.

C. Dependence on Exchange

The commonly used statistical exchange approximation suffers from uncertainties as to the best form to be used. This uncertainty is expressed in the parameter α, which multiplies the $\rho^{1/3}$ term of the exchange operator: $\alpha = 1$ is known as Slater's value of exchange and frequently yields better eigenvalues than the more formally correct term, for which $\alpha = \frac{2}{3}$, as taken from the work of Gaspar[27] and Kohn and Sham.[26] In many instances α is now taken to be a variational parameter ($\frac{2}{3} \leq \alpha \leq 1$)—as described at length by Slater and associates in several recent papers.[29] The higher values for α normally occur in the more inhomogeneous and lower-*Z* (atomic number) systems,[30] where the assumptions of the statistical approximations are not valid.

This form of exchange approximation is admittedly crude and acceptable in the lighter elements because of a fortunate coincidence. In the worst case, that of a transition-metal band structure, the plane-wave (or "*s*-like") bands are fairly insensitive to exchange and so the position of the more sensitive *d* bands can be properly placed by adjusting the value of α, and the resulting band structure usually agrees well with experiment. For the rare-earth metals, the unfilled 4*f* states are localized (atomic) in character and so do not belong in a conduction-electron band structure, which then resembles closely that of a transition metal. [Further, the 5*d* and "6*s*-*p*" bands of the rare earths apparently hybridize so strongly that the variation of α only shifts the positions of the bands in the same direction (up or down in energy) rather than relative to each other.] As we shall see for uranium metal, the 6*d* bands are found to be very broad and less sensitive (but not insensitive) to the exchange approximation. The 5*f* states, however, are sensitive to the choice of α, with their relative position changing by about 0.25 Ry in going from $\alpha = \frac{2}{3}$ to $\alpha = 1$.

III. RESULTS OF THE CALCULATION

A. Relativistic Band Structure of bcc Uranium

As indicated in Sec. II, we have done a number of detailed WMT calculations on bcc uranium, its high-temperature structure, using various choices of atomic configurations (cf. Fig. 1) to make up the crystal potentials in the WMT approximation, and have varied α, the exchange constant. The lattice parameter was taken to be 6.5649 a.u. and the sphere radius 2.8062 a.u. The calculations are accurate to 1 mRy. A total of 150 to 200 inequivalent points per band in the zone were determined. These were Fourier-series fit to determine $N(E_F)$ and E_F using the QUAD linear procedure.[31]

The effect of changing the atomic configuration on the resulting band structure is shown in Fig. 2, for the three atomic configurations represented earlier in Fig. 1, namely, f^4s^2, $f^3d^1s^2$, and $f^2d^2s^2$. Here the bands along the high-symmetry directions are shown for the choice $\alpha = 1$. The energy region of the 5*f* asymptotes is shown shaded for the $f^2d^2s^2$ configuration. (Asymptotes arise in the APW scheme whenever the radial wave function has its zero at the sphere radius, in which case the corresponding logarithmic derivative goes through a singularity.) Since for uranium metal only few bands have been found which cross the asymptote regions, we have not gone to the trouble of determining the actual band structure across this range of energy.

The atomic character or symmetry of the bands is best seen at Γ: starting with the lowest band, Γ_6^+, which corresponds to the bottom of the "*s*-like" band, the next bands are the *f* bands (at Γ_7^- and Γ_8^-), then both *d*-like (Γ_8^+ and Γ_7^+) and *f*-like bands (Γ_8^- and Γ_6^-) in various orders depending on configuration. The upward motion in energy (with increasing number of 5*f* electrons, i.e., 2, 3, or 4, in the assumed starting configuration) is evident and shows the self-consistency effect in operation. The position ordering of the bands appears to be what is expected from the atomic characteristics discussed above. The hybridization of the 5*f* bands with the "7*s*-*p*" and 6*d* bands is clearly evident [cf. results in Fig. 2(b) for the $f^3d^1s^2$ calculation], but the bands, particularly the lowest 5*f* bands [of Fig. 2(b) especially], appear to be flatter than expected and, as we shall see, are found for the $\alpha = \frac{2}{3}$ band structures.

Three band-structure calculations were performed for the three different assumed starting potentials but with $\alpha = \frac{2}{3}$; these are shown in Fig. 3. Here we see the same level-ordering scheme as found in the $\alpha = 1$ calculations, but the results—particularly for the $f^3d^1s^2$ configuration—appear more physically correct and closer to our expectation of self-consistency.

The strong hybridization of the 5*f* bands with the very broad "7*s*-*p*" and broad 5*d* bands is clearly evident, as is the upward movement of the 5*f* bands as in the number of 5*f* electrons in the assumed atomic potential (2, 3, or 4) is increased. The relative insensitivity of the three band structures shows that the Coulomb correlation for these *f* electrons is smaller than the effective bandwidth, and confirms the applicability of the band model to the lower actinides. (The applicability of the band model for the heavier actinides be-

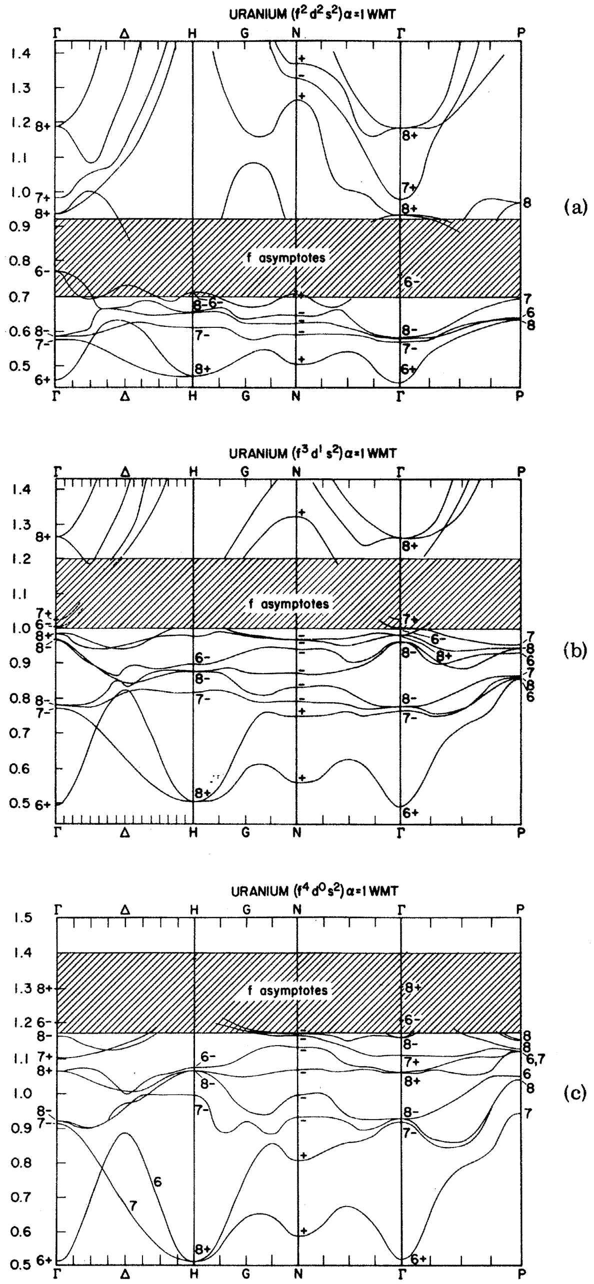

FIG. 2. Energy bands (in rydbergs) resulting from the three diffferent starting-potential configurations are shown for full Slater exchange. The shaded region indicates the *f*-asymptote energy range. (See text for explanation.)

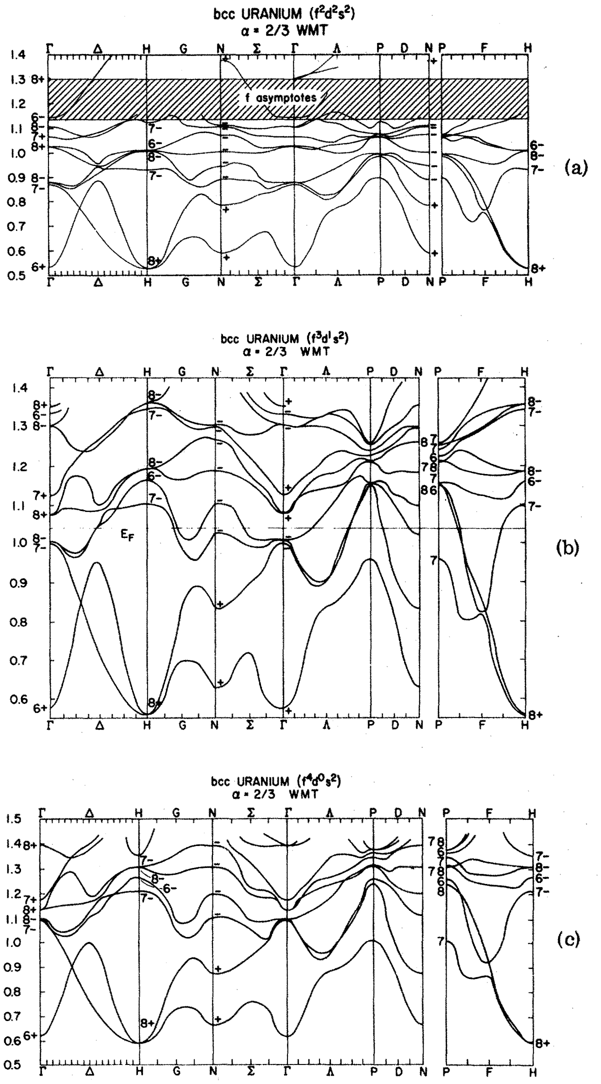

FIG. 3. Energy bands (in rydbergs) resulting from the three different starting-potential configurations are shown for the Kohn–Sham–Gaspar exchange. The shaded region indicates the f-asymptote energy range. (See text for explanation.)

comes questionable with increasing atomic number.) This choice of α ($=\frac{2}{3}$) is also close to the value (0.69) expected from nonrelativistic X_α calculations for the free atoms.[30]

Some of the essential features of the band structures obtained with the two values of α and the three atomic starting configurations are best seen in the summary of results given in Table I. With the zero of energy in each calculation taken as the value for Γ_6^+ (the bottom of the "7s-p"-like band), we list the two lowest Γ_8^+ eigenvalues (giving the crystal field splitting of the d bands), the H_8^+ value (which gives the lowest part of the d band), and the lowest Γ_7^- (which gives the position of the lowest f band relative to the plane-wave band). Looking first at the Γ_7^- values, we see the upward motion in energy of the f bands with increasing f character in the assumed configuration, as previously mentioned. The underlying structure of the s-d bands (cf. Γ_8^+, Γ_8^+, and H_8^+) is remarkably unchanged by both the change of 5f configuration and the change in the exchange parameter α. The greater sensitivity of the position of the 5f bands in the $\alpha = 1$ case reflects the occupation-number dependence which results whenever the Coulomb correlation energy is important. (The 5f orbitals for $\alpha = 1$ are more spatially localized—a trend that becomes increasingly important as one proceeds to the heavier actinides.)

The shifting upward of the f bands found for $\alpha = \frac{2}{3}$ relative to $\alpha = 1$ leaves the "s-d" bands relatively undisturbed and results in (i) greater overlap of the f orbitals and (ii) stronger hybridization (especially with the d bands) and hence effectively wider "f" bands than in the case of the $\alpha = 1$ bands. We have attempted to give some index of the width of the f bands by giving the energy separation of the Γ_7^- and the two f asymptotes labeled W_f. Since the upper asymptote occurs about 0.1 Ry above the top of the f band, this is an upper bound on the width of the f bands. As it appears that the lower asymptote occurs very near the top of the bands, this is a reasonable estimate of the width.

As a further test of our results and because it provides a better understanding of the effects of the 5f states, we have calculated the band structure which would exist for γ-uranium if the f bands were entirely absent from the range of energy in which we have found the "7s-p"-like bands and the 6d bands. Such a calculation is easily done by shifting in energy the logarithmic derivatives for the f electrons. The results of this unrealistic calculation are presented in Fig. 4. Comparing these results with the bands of a high-atomic-number fcc transition metal, such as tungsten,[32] we see that the bands of Fig. 4 are those of a typical transition metal. There is the free-electron band which begins with the Γ_6^+ state and then rises rap-

TABLE I. Selected data from the six different calculations of the γ-uranium band structure. (Energy in rydbergs.)

	$\alpha=\frac{2}{3}$			$\alpha=1$		
	f^2	f^3	f^4	f^2	f^3	f^4
Γ_8^+	0.493	0.507	0.514	0.490	0.487	0.548
Γ_8^+	0.769	0.773	0.772	0.742	0.767	0.783
H_8^+	−0.005	−0.019	−0.030	+0.019	+0.009	−0.002
Γ_7^-	0.336	0.426	0.471	0.128	0.275	0.395
W^f	0.651	0.827	0.937	0.316	0.525	0.723
	0.730	0.903	1.012	0.404	0.610	0.804

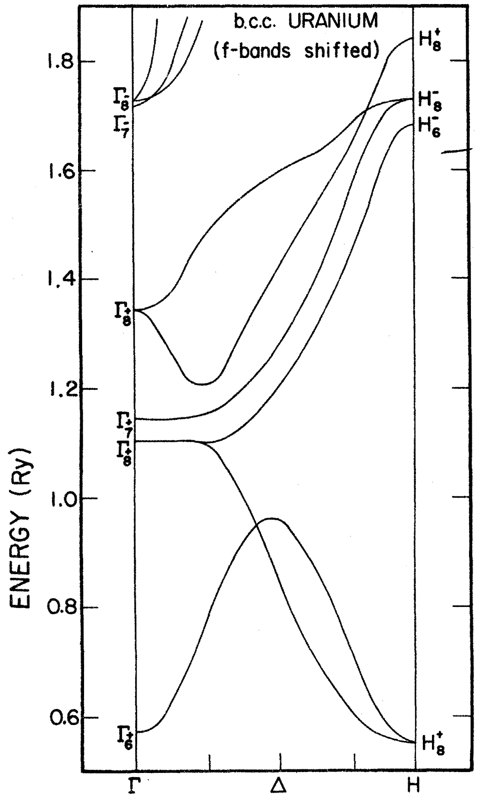

FIG. 4. Energy band structure which results if the f states are arbitrarily moved out of range. (Energy in rydbergs.)

idly. Cutting across this band and hybridizing with it are the d bands consisting of the $\Gamma_8^+ - \Gamma_7^+$ spin-orbit-split states and the higher Γ_8^+ state. These are broad d bands with the descending bands coming down to the energy region of the Γ_6^+. Several bands have interacted via the spin-orbit coupling to form anticrossings where there would have been crossings in the nonrelativistic bands. The real band structure, with the $5f$ states included as in Fig. 3(b), is now more readily understood as that of a transition metal with $5f$ bands superposed onto the s-d bands and strongly hybridized with them.

Finally, we need to discuss the role of relativistic effects and to make comparisons with nonrelativistic energy band structures which have been reported. The importance of relativistic effects for describing the properties of the actinides was emphasized quite early in the study of these elements.[9] These change the nonrelativistic results in a number of significant ways of which the most important are the following: The states are split in energy by the spin-orbit interaction by an amount which is usually larger than the crystal field splittings for the $5f$ electrons, and the orbitals of lower angular momentum are shifted downward relative to the higher-angular-momentum states. This latter effect is graphically shown in Figs. 1–3 of Lehman[9] and Table I of Boyd, Larson, and Waber.[33] To further illustrate this effect, we have tabulated in Table II the relativistic[34] and nonrelativistic[35] atomic eigenvalues for uranium in the $5f^3d^1s^2$ configuration using KSG exchange. In the nonrelativistic calculation, the $7s$ states are found to lie 0.4 Ry *above* the $5f$ state, while in the relativistic calculation they are 0.1 Ry *below* the $5f$ energy. Similarly, the $7s$ are (barely) above the $6d$ in the nonrelativistic calculation and about 0.15 Ry below in the relativistic one. Such an effect is certainly present for Pu, as pointed out by Kmetko and Waber.[36] Furthermore, the relativistic $5f$ orbitals are expanded spatially relative to the nonrelativistic ones by roughly 20% (due to the relativistic contraction of the core states which in turn causes increased screening of the nuclear charge). It is therefore not surprising that nonrelativistic energy-band calculations give only a crude representation of the band structure of the actinide metals.

In order to make detailed comparisons, we have calculated the energy band structure of U metal in the nonrelativistic limit. These results, shown as Fig. 5 for the bands along Γ-H, agree with nonrelativistic results reported earlier[15,16] and are *incorrect* in a number of ways. The ordering and separations of the bands are incorrect; the bottom of the $7s$-like bands (the Γ_1 state) lies above the $5f$ bands and the lowest state at point H is found to be far below the Γ_1 state. The large spin-orbit splittings of the bands are missing and degeneracies have not been removed causing crossing of bands rather than anticrossings. Finally, the relativistic effect causing $5f$ orbital expansion is absent, and hence estimates of $5f$ bandwidths or electronic charge within the APW spheres are doubtful. All these

TABLE II. Comparison of atomic energy levels from relativistic and nonrelativistic calculations. (Energy in rydbergs.)

	Relativistic		Nonrelativistic	
	$\alpha=\frac{2}{3}$	$\alpha=1$	$\alpha=\frac{2}{3}$	$\alpha=1$
$5f^3_{5/2}$	0.1635	0.5698	0.6372	1.1830
$5f^0_{7/2}$	0.1046	0.4982	0.6372	1.1830
$6s^2_{1/2}$	3.4499	3.8298	2.5631	3.0399
$6p^2_{1/2}$	2.1062	2.4422	1.5593	1.9181
$6p^6_{3/2}$	1.4501	1.7390	1.5593	1.9181
$6d^1_{3/2}$	0.1243	0.2949	0.2136	0.4494
$6d^0_{5/2}$	0.0911	0.2493	0.2136	0.4494
$7s^2_{1/2}$	0.2603	0.3803	0.2046	0.3530

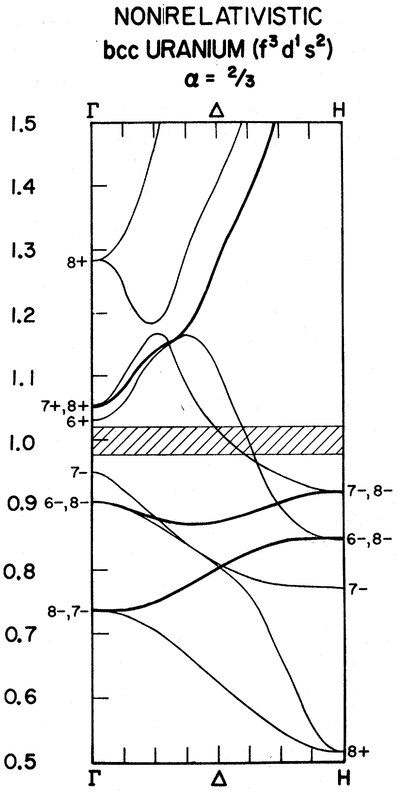

FIG. 5. Nonrelativistic energy-band calculation for γ-U. (Energy in rydbergs.)

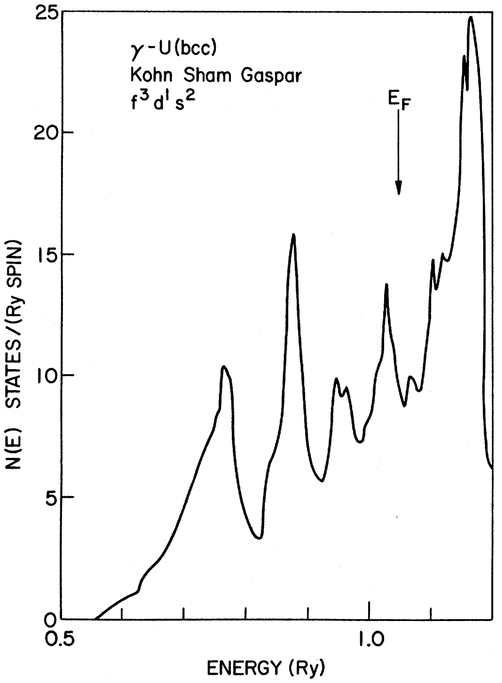

FIG. 6. Density of states for the potential resulting from ($f^3d^1s^2$) configuration and Kohn–Sham–Gaspar exchange.

differences make questionable the value of any nonrelativistic band result for the actinide metals.

B. Density of States and Fermi Surface

The position of the Fermi energy (at 1.047 Ry) is given for the $f^3d^1s^2$ potential [Fig. 3(b)] as this is the configuration considered to be the best choice for the starting potential. We have calculated the density of states $N(E)$, shown in Fig. 6 for this band structure. It shows considerable structure as would be expected for a set of s-p, d, and f bands all hybridizing with each other. Note in particular the large peak in $N(E)$ at about 1.17 Ry and the large absorption peak to be expected for optical transitions at 0.3 Ry (i.e., at about 4 eV). The density of states at the Fermi energy is found to be 1.45 states/atom eV. Unfortunately, no low-temperature specific-heat measurements are available. However, such a high value is quite consistent with the large electronic specific heats of the actinides.[37] The electronic specific heat for α-U would, in fact, correspond to an $N(E_F)$ of more than 4 states/atom eV if one neglects electron-phonon enhancements.

Figure 7 shows the Fermi surface resulting from this potential as it crosses the various planes bounding the irreducible $\frac{1}{48}$th wedge of the Brillouin zone (see Fig. 8). It exhibits hole surfaces from the second and third bands and an electron surface from the fourth band. These different surfaces are indicated by different cross hatchings. This Fermi surface is a highly tentative one as changes in potentials will move the f bands relative to the spd band structure and this will change the shape of the Fermi surface; this picture is presented as a possible guide for the interpretation of

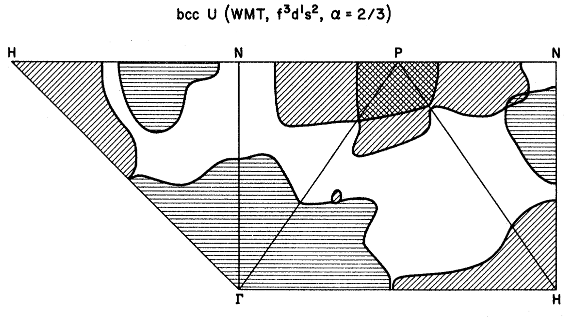

FIG. 7. Intersection of the Fermi surface with the planes bounding irreducible $\frac{1}{48}$th wedge of the Brillouin zone (cf. Fig. 8). The fourth-band electron surfaces have been shown with horizontal hatching. The hole surfaces from the second and third bands have been shown with diagonal hatching in opposite directions. Because the second-band holes occur entirely within the third-band hole surface at P, this results in cross hatching in the second-zone area.

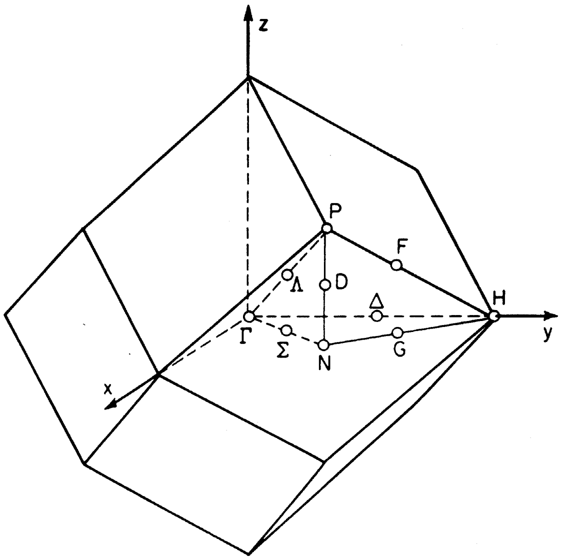

FIG. 8. Brillouin zone for a bcc lattice showing the irreducible wedge.

positron-annihilation experiments now under way on this system.[38]

IV. DISCUSSION

The work presented here is but one further initial step toward an understanding of the electronic structure of the actinide metals. Much remains to be done both experimentally and theoretically. The most significant feature to be seen from the calculations is that the f states do have sizable bandwidths and, although they are sensitive to the potential, they hybridize with a rather stable (i.e., insensitive to potential) transition-metal-like set of bands. To further illustrate the bandlike behavior of the f-character electrons, we show in Fig. 9 the radial charge density of the f character ($l=3$ part of the wave function) at several energies throughout the band-structure range. Only the shapes are significant in these pictures, so all labels have been suppressed. If one now looks at the energy corresponding to the bottom of the $7s$-p bands (~0.6 Ry), the radial charge density clearly corresponds to a plane wave orthogonalized to a core. As one moves up in energy, this OPW-like character dies away and the charge density looks more like that from a tight-binding system. Only when one arrives at the top of the f-state region—or perhaps a bit above it—does one find the charge density looking like an atomic $5f$ confined to a single site. This appears to be a very convenient graphic way to appreciate the itinerant character of the f states in this system.

As mentioned in the Introduction, there is considerable speculation as to the nature of the $5f$ electrons in both α- and γ-uranium.[4] From the charge densities shown in Fig. 9, it is clear that in γ-U the $5f$ states at or below the Fermi energy have little resemblance to atomic $5f$ orbitals. Their strongly itinerant nature would therefore in no way tend to "suppress" superconductivity (the role postulated for the localized $5f$ electrons) as has been suggested by Geballe *et al.*[39] for γ-U. The nature and role of the $5f$ electrons in superconductivity awaits detailed band calculations (now in progress[40]). The calculation of the electron-phonon interaction in γ-U would be illuminating, particularly in establishing the role of the $5f$ vs the $6d$ electrons. The results presented here, including the available crystal wave functions, make such a calculation feasible (if still computationally difficult to perform).

Finally, the absence of magnetic ordering in uranium metal may be readily understood qualita-

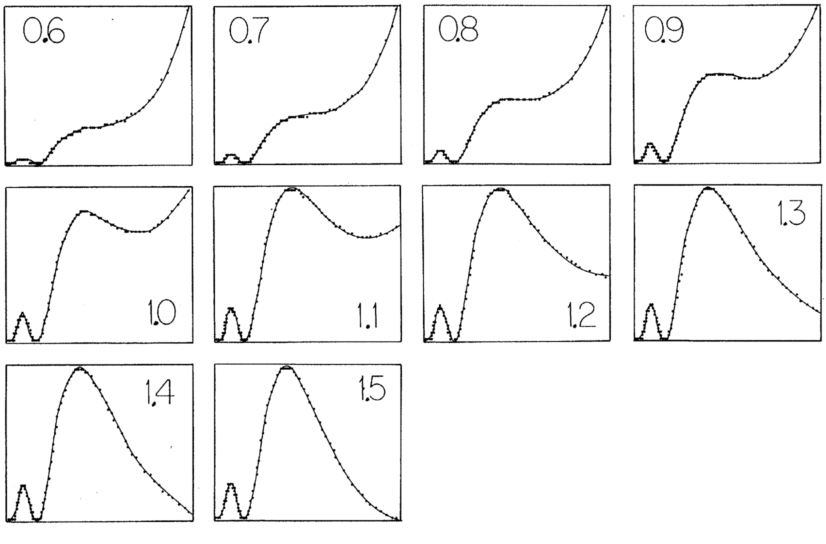

FIG. 9. Radial charge densities of the $\kappa=3$ component at various energies through the energy range of the band structure. As only shapes are significant here, neither of the axes is labeled. The radial distance (on the horizontal axis) is linear with $0\le R\le R_{\mathrm{MT}}=2.8062$ a.u. The "normalization" of the charge density is determined by the requirement that the plot just fill the frame.

tively from our band results. The strong hybridization of the broad 5*f* itinerant states with the very broad 6*d*-7*s* bands results in a band structure which has an over-all large effective bandwidth for the (possible) magnetic carriers. This makes it energetically too costly to produce any magnetization (flipping of spins); i.e., in the band picture[41] the kinetic-energy penalty of promoting an electron of one spin band into the opposite spin band exceeds the lowering of energy due to exchange interactions (because the effective width is just too great). We expect this same qualitative picture to hold for all the lighter actinide metals, which also show no magnetic ordering.

ACKNOWLEDGMENT

We are grateful to Miss Sue Katilavas, Applied Mathematics Division, Argonne National Laboratory, for computational assistance.

---

[*] Supported by the U. S. Atomic Energy Commission, the Air Force Office of Scientific Research, and the National Science Foundation.

[†] Present address: Argonne National Laboratory, Argonne, Ill. 60439.

[1] For an early general review, see G. T. Seaborg, in *The Actinide Elements*, edited by G. F. Seaborg and J. J. Katz (McGraw-Hill, New York, 1954), p. 733.

[2] For a more recent review of the field, see *Plutonium 1970 and Other Actinides*, edited by W. N. Miner (AIME, New York, 1970).

[3] B. T. Matthias and G. T. Geballe, Science **151**, 985 (1966).

[4] H. H. Hill, R. W. White, and B. T. Matthias, Phys. Rev. **163**, 356 (1967), and references therein.

[5] J. W. Ross and D. J. Lam, Phys. Rev. **165**, 617 (1968) (α-U).

[6] W. E. Gardner and T. F. Smith, Phys. Rev. **154**, 309 (1967) (α-U).

[7] J. Friedel, J. Phys. Chem. Solids **1**, 175 (1956).

[8] G. W. Lehman, *Metallurgy and Fuels*, edited by J. P. Howe and H. M. Finniston (Addison-Wesley, Reading, Mass. 1958), Vol. II, p. 570.

[9] G. W. Lehman, Phys. Rev. **116**, 846 (1959); Phys. Rev. **117**, 1493 (1960).

[10] E. Cicely Ridley, Proc. Phys. Soc. Lond. A **247**, 199 (1958).

[11] A. J. Freeman and D. D. Koelling, Bull. Am. Phys. Soc. **14**, 360 (1969); G. O. Arbman, D. D. Koelling, and A. J. Freeman, Bull. Am. Phys. Soc. **15**, 344 (1970); D. D. Koelling, A. J. Freeman, and G. O. Arbman, in Ref. 2, p. 194.

[12] D. D. Koelling, A. J. Freeman, and F. M. Mueller, Phys. Rev. B **1**, 1318 (1970).

[13] T. Loucks, *The Augmented Plane Wave Method* (Benjamin, New York, 1967).

[14] D. D. Koelling, Phys. Rev. **188**, 1049 (1969).

[15] E. A. Kmetko, *Electronic Density of States*, Nat. Bur. Stand. Spec. Publ. No. 323 (U.S. GPO, Washington, D. C., 1971), p. 67.

[16] E. A. Kmetko and H. Hill, in Ref. 2, p. 233.

[17] L. F. Mattheiss, Phys. Rev. **133**, 184 (1963); Phys. Rev. **134**, A1399 (1964).

[18] F. S. Ham and B. Segall, Phys. Rev. **124**, 1786 (1961).

[19] R. S. Leigh, Proc. Phys. Soc. Lond. **71**, 33 (1957); P. M. Marcus, Intern. J. Quantum Chem. **1**, 567 (1967).

[20] P. DeCicco, Phys. Rev. **153**, 931 (1967).

[21] W. Rudge, Phys. Rev. **181**, 1020 (1969); Phys. Rev. **181**, 1024 (1969).

[22] L. F. Mattheis, Phys. Rev. **181**, 987 (1969).

[23] F. Beleznay and M. J. Lawrence, J. Phys. C **1**, 1288 (1968).

[24] P. DeCicco and J. C. Slater, MIT Solid State and Molecular Theory Group Quarterly Progress Report No. 50, p. 46, 1963 (unpublished).

[25] J. C. Slater, Phys. Rev. **81**, 385 (1951).

[26] W. Kohn and L. J. Sham, Phys. Rev. **140**, A1133 (1965).

[27] R. Gaspar, Acta Math. Acad. Sci. Hung. **3**, 263 (1954).

[28] See review by A. J. Freeman, in *Magnetism in the Rare Earth Metals*, edited by R. J. Elliot (Plenum, New York, 1972).

[29] J. C. Slater and K. H. Johnson, Phys. Rev. B **5**, 844 (1972).

[30] E. A. Kmetko, Phys. Rev. A **1**, 37 (1970).

[31] J. F. Cooke and R. F. Wood, Phys. Rev. B **5**, 1276 (1972); see also F. M. Mueller, J. W. Garland, M. H. Cohen, and K. H. Bennemann, Ann. Phys. (N.Y.) **67**, 19 (1971).

[32] L. F. Mattheiss and R. E. Watson, Phys. Rev. Lett. **13**, 526 (1964); L. F. Mattheiss, Phys. Rev. **139**, A1893 (1965); T. L. Loucks, Phys. Rev. **143**, 506 (1966); I. Petroff and C. R. Viswanathan, Phys. Rev. B **4**, 799 (1971).

[33] R. G. Boyd, A. C. Larson, and J. T. Waber, Phys. Rev. **129**, 1629 (1963).

[34] D. Liberman, J. T. Waber, and D. T. Cromer, Phys. Rev. **137**, 27 (1965).

[35] F. Herman and S. Skillman, *Atomic Structure Calculations*, (Prentice-Hall, Englewood CLiffs, N. J., 1963).

[36] E. A. Kmetko and J. T. Waber, in *Proceedings of the Third International Conference on Plutonium, London, 1965* (Chapman and Hall, London, 1967).

[37] J. A. Lee, P. W. Sutcliffe, D. J. Martin, and K. Mendelssohn, in Ref. 2, p. 58.

[38] W. Triftshäuser (private communication).

[39] T. H. Geballe, B. T. Matthias, K. Andres, E. S. Fisher, F. Smith, and W. H. Zachariasen, Science **152**, 755 (1966).

[40] D. D. Koelling and A. J. Freeman (unpublished).

[41] J. C. Slater, Phys. Rev. **49**, 537 (1936); Phys. Rev. **49**, 931 (1936); Phys. Rev. **52**, 198 (1937).